

Supporting information

**Reliable discrimination of histamine and ethylenediamine in meat samples using
colorimetric affordable test strip (CATS): Introducing a novel lab-on paper strategy for
low-cost ensuring food safety by rapid and accurate monitoring of biogenic amines**

Arezoo Saadati ^a, Fatemeh Farshchi ^b, Mohsen Jafari ^c, Houman Kholafazad ^d, Mohammad
Hasanzadeh ^{e,*}, Nasrin Shadjou ^f

^a Nutrition Research Center, Tabriz University of Medical Sciences, Tabriz, Iran.

^b Fundação Oswaldo Cruz, Instituto Oswaldo Cruz, Laboratório de Biologia Molecular e Doenças Endêmicas, Avenida Brasil No 4365-Manguinhos, Rio de Janeiro 21040-900, RJ, Brazil.

^c Biotechnology Research Center, Tabriz University of Medical Sciences, Tabriz, Iran.

^d Food and Drug Safety Research Center, Tabriz University of Medical Sciences, Tabriz, Iran.

^e Pharmaceutical Analysis Research Center, Tabriz University of Medical Sciences, Tabriz, Iran.

^f Department of Nanotechnology, Faculty of Chemistry, Urmia University, Urmia, Iran.

Corresponding Author

* (Mohammad Hasanzadeh) Pharmaceutical Analysis Research Center, Tabriz University of Medical Sciences, Tabriz, Iran.

E-mail address: (*) hasanzadehm@tbzmed.ac.ir

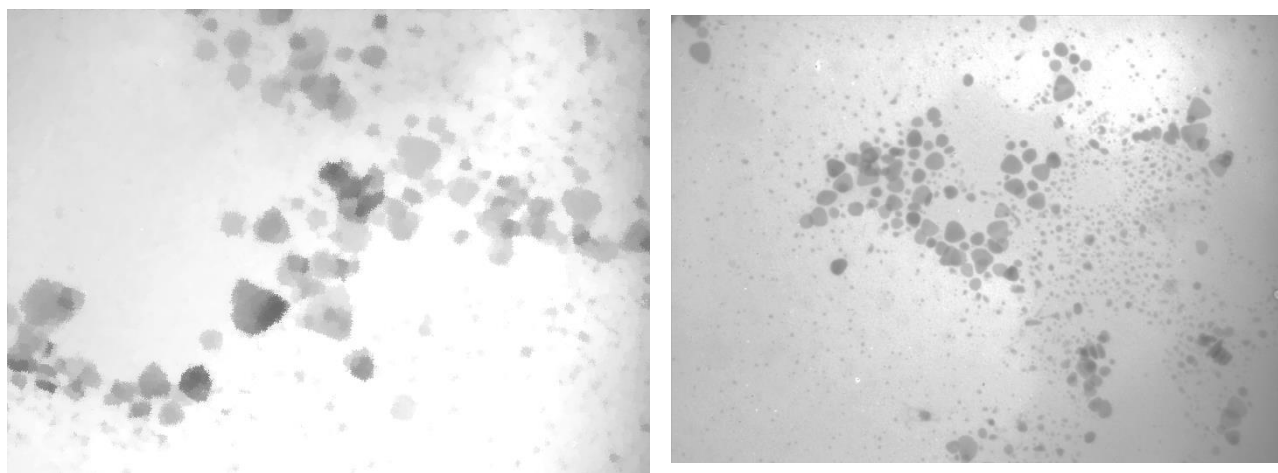


Fig. S1. A) TEM images of AgNPs in two magnifications (included with permission [32]).

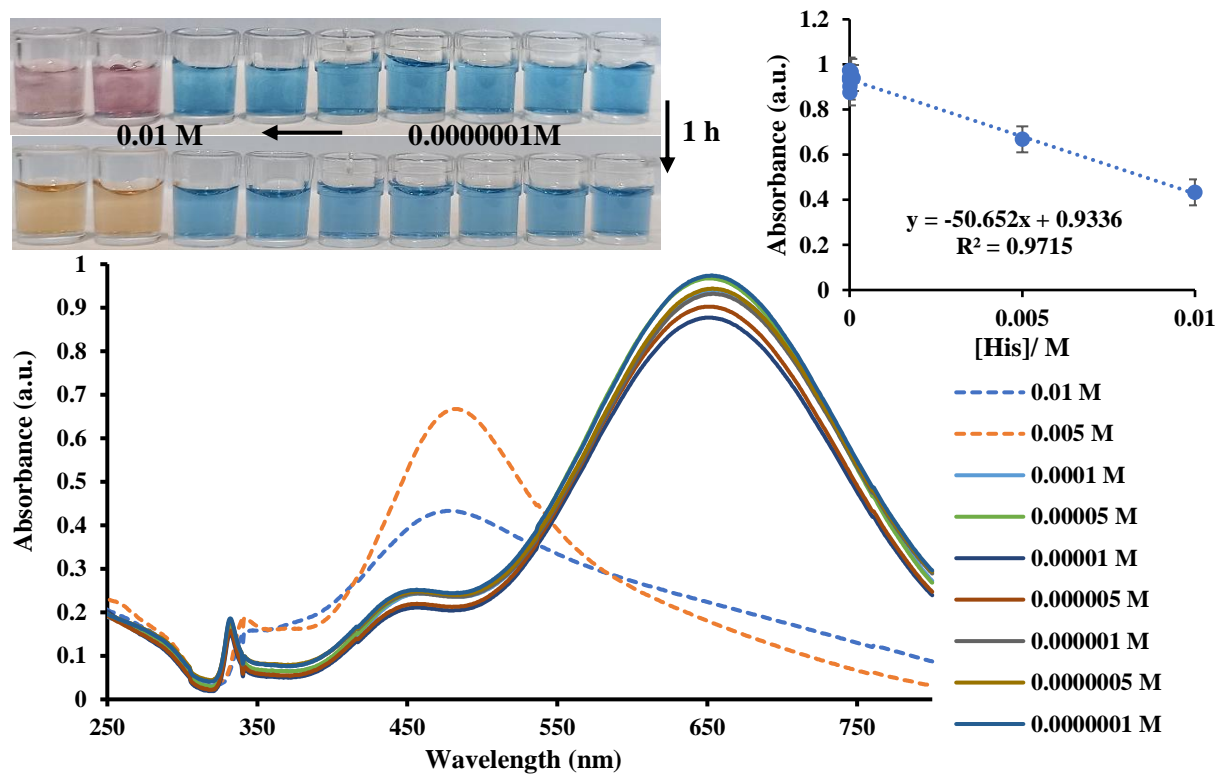


Figure S2. A) The UV-Vis spectra of AgNPs in the presence of various concentration of HIS. Inset; Calibration curve.

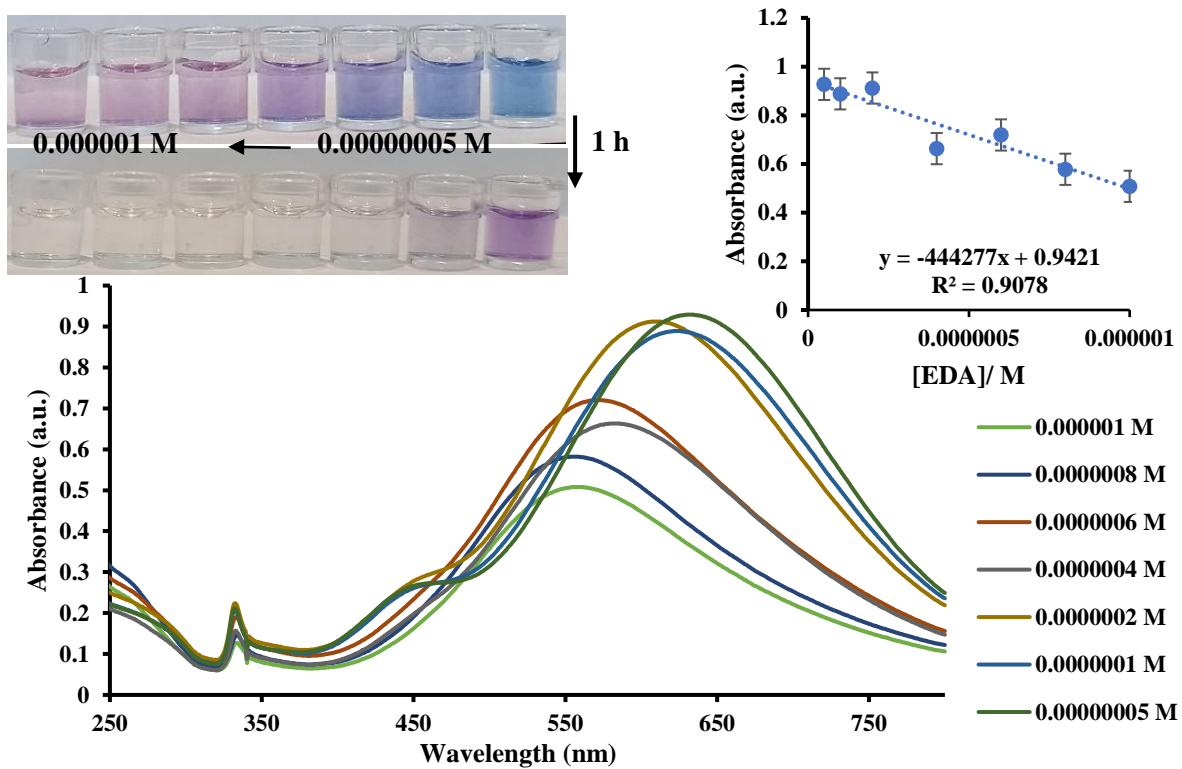
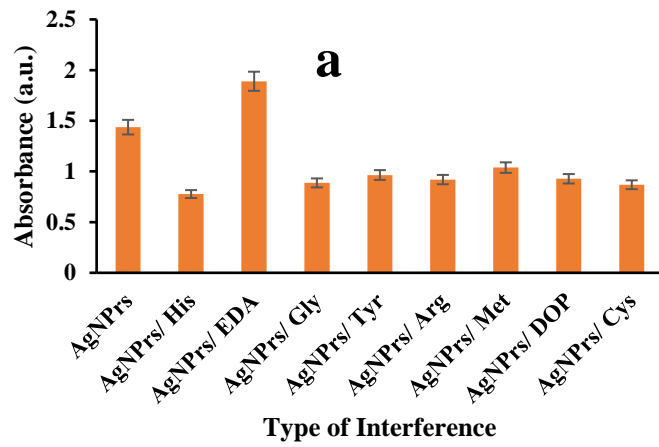
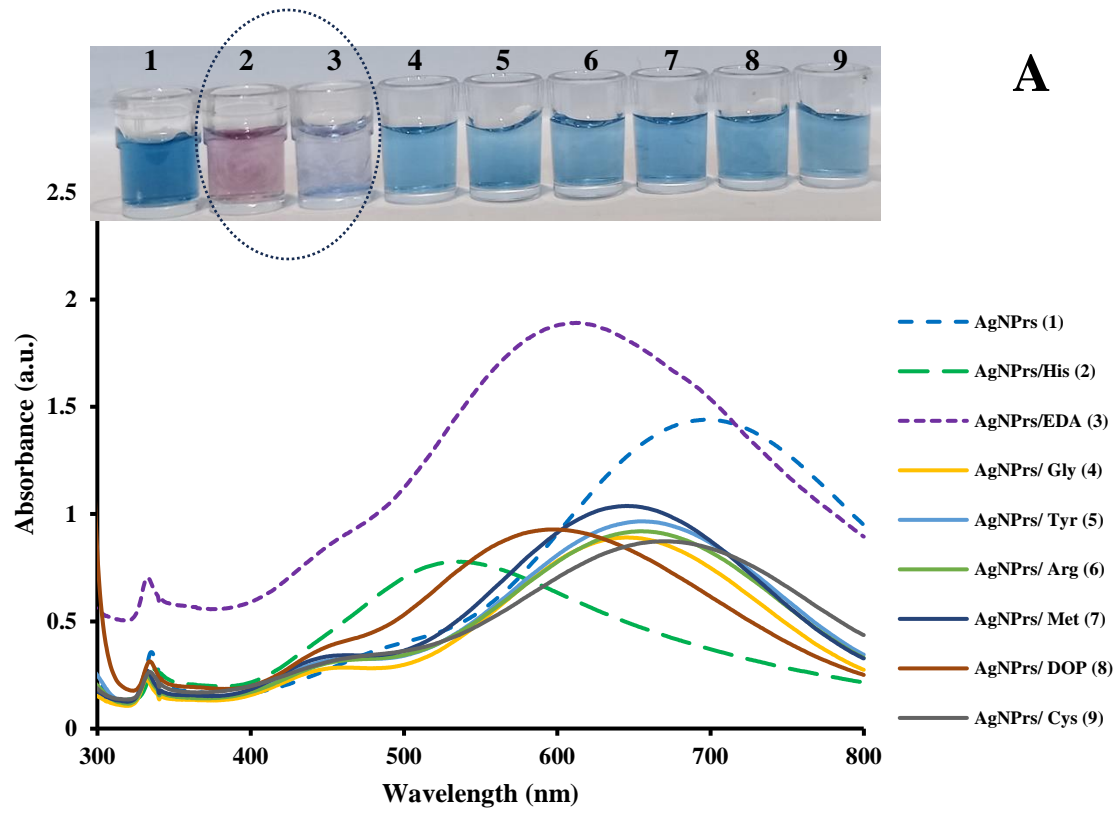
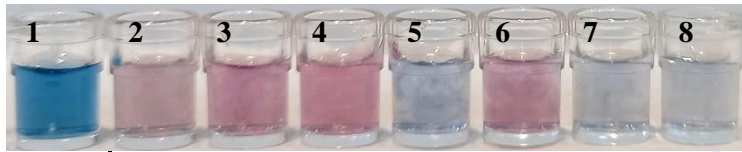
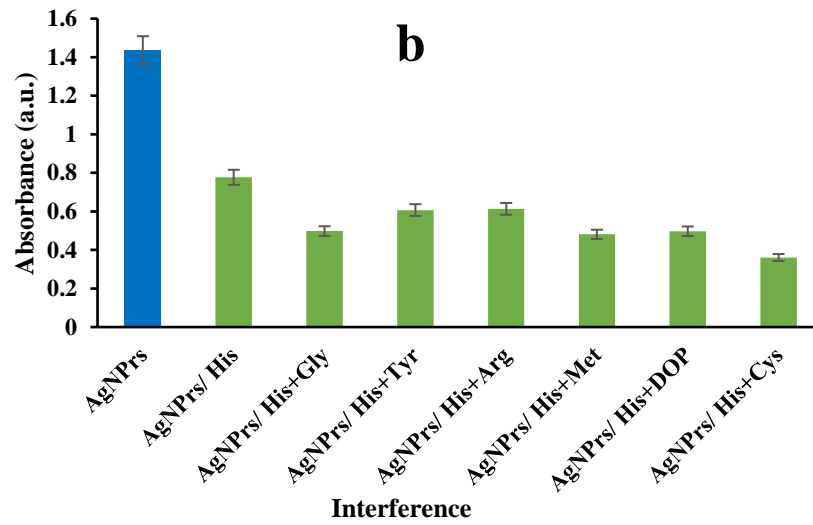
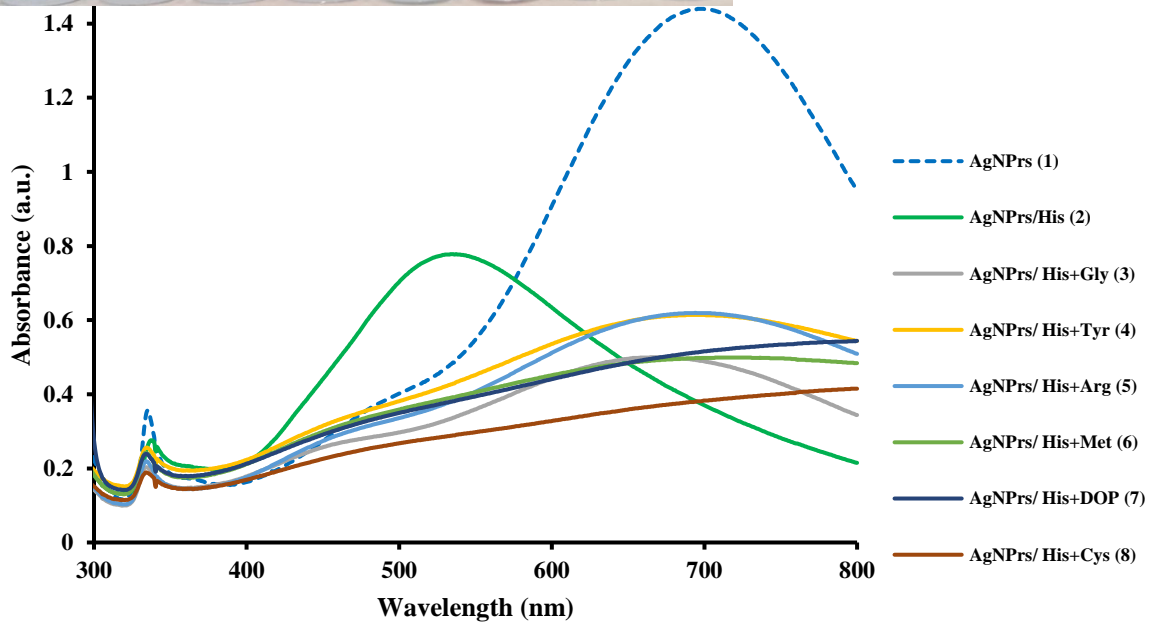


Figure S3. A) The UV-Vis spectra of AgNPs in the presence of various concentration of EDA. **Inset;** Calibration curve.





B



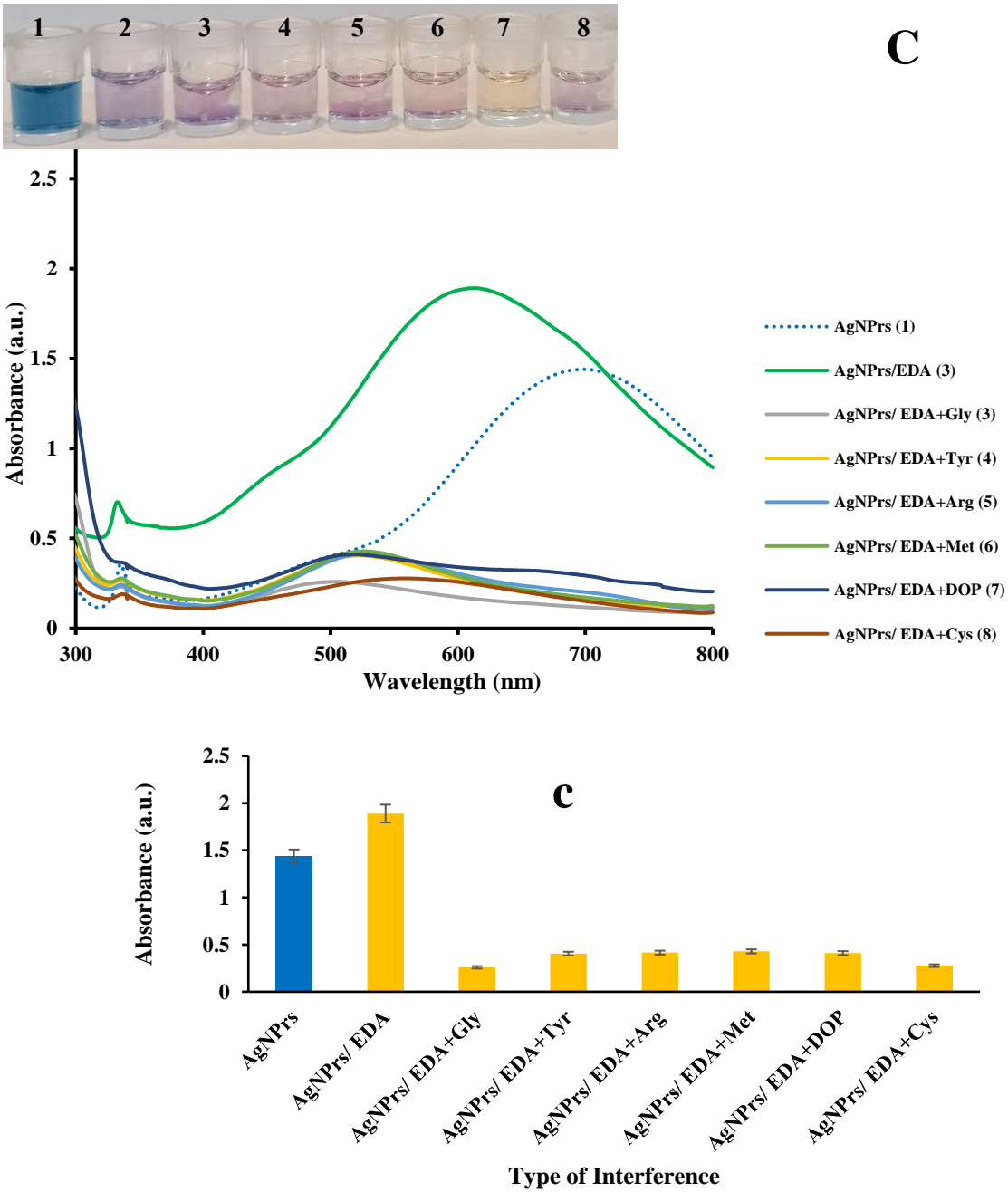
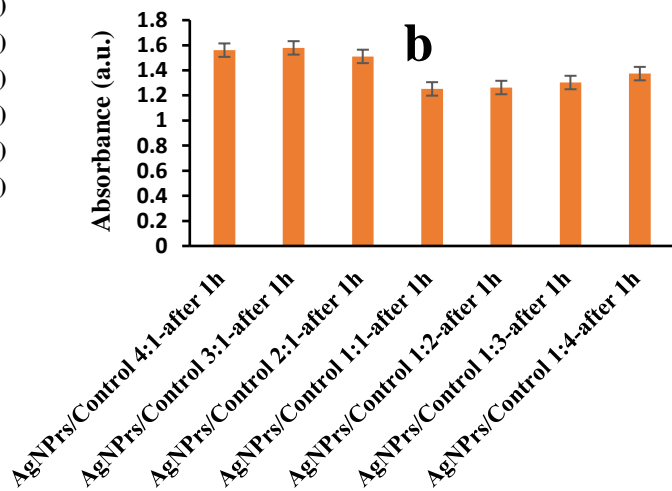
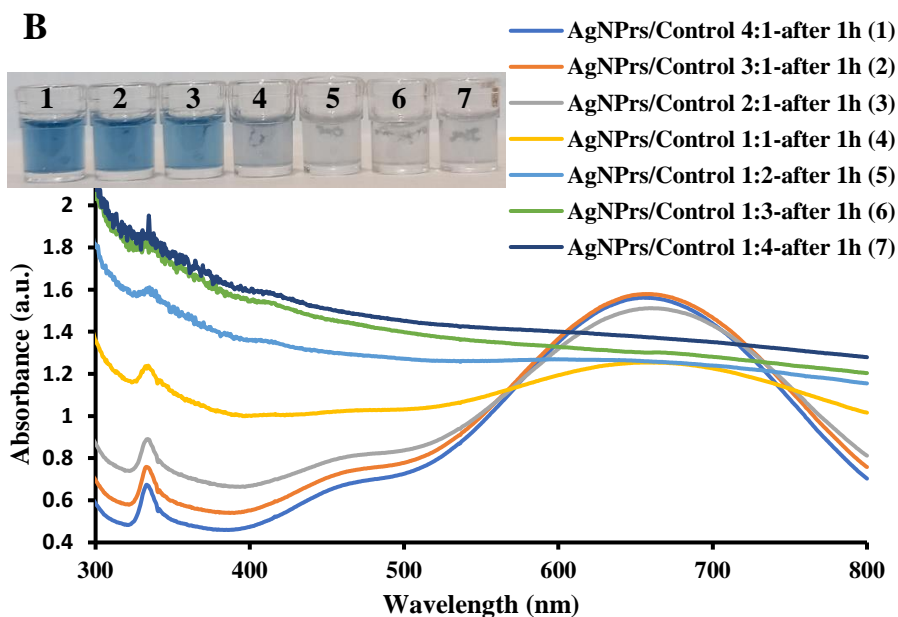
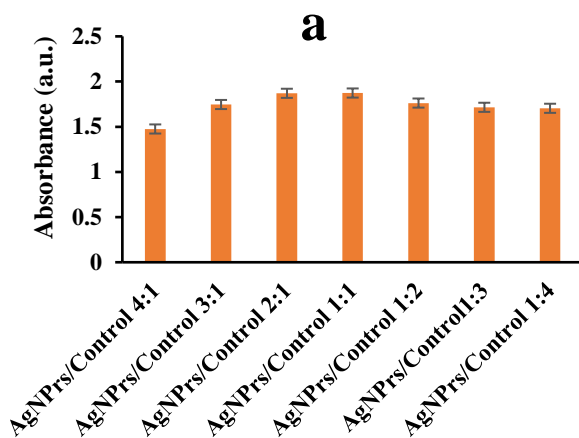
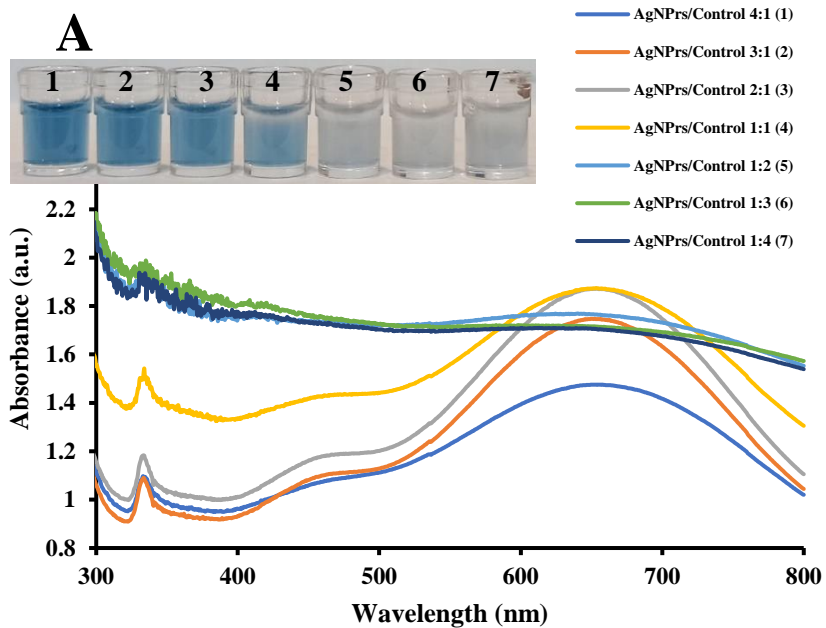
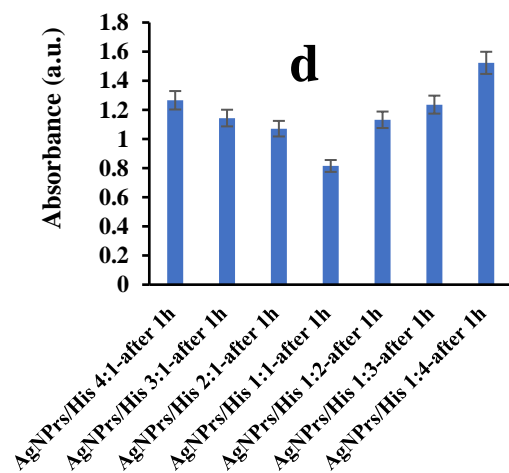
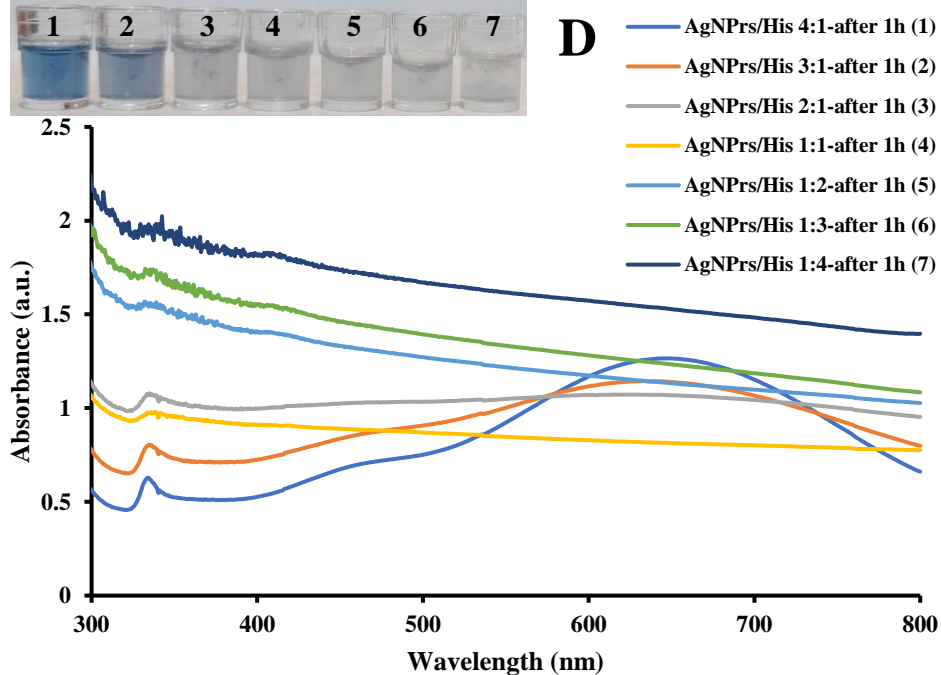
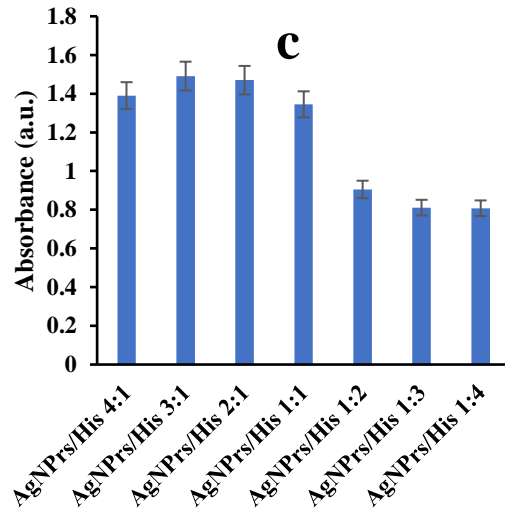
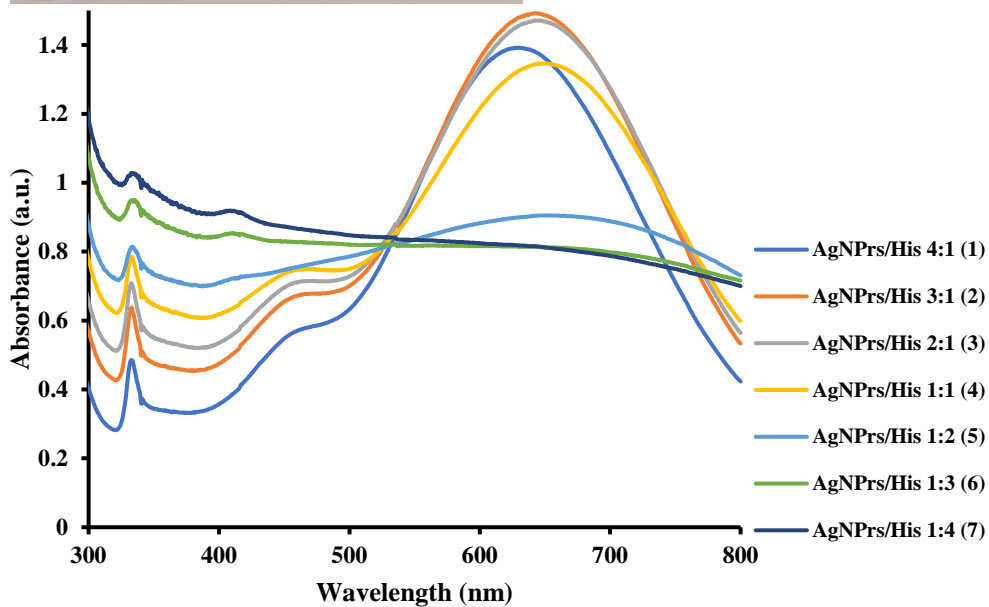


Figure S4. Selectivity of optical chemosensor to detection of EDA and HIS in the presence of various interferences (A), His in the presence of interferences (B), EDA in the presences of EDA (C).





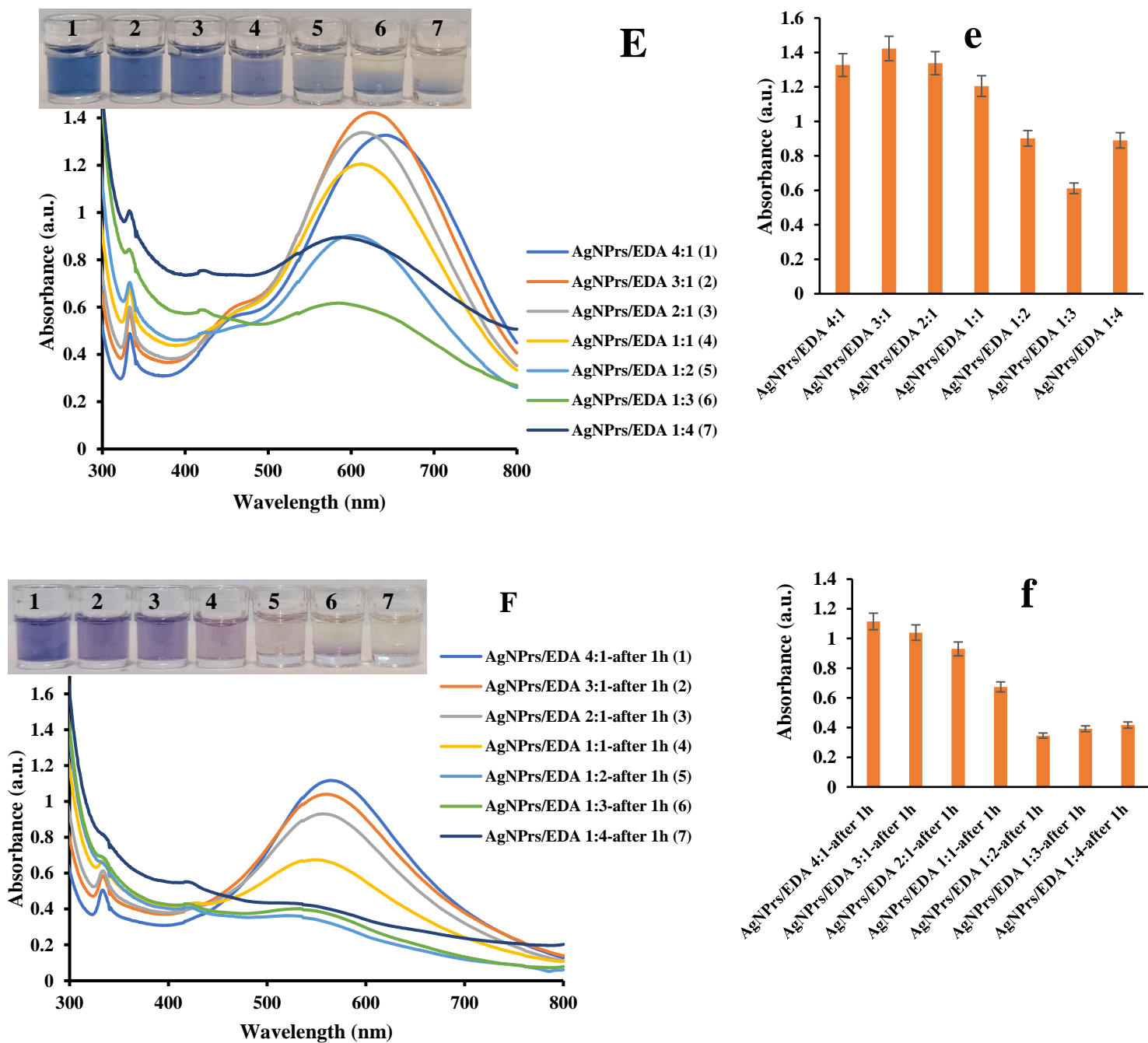
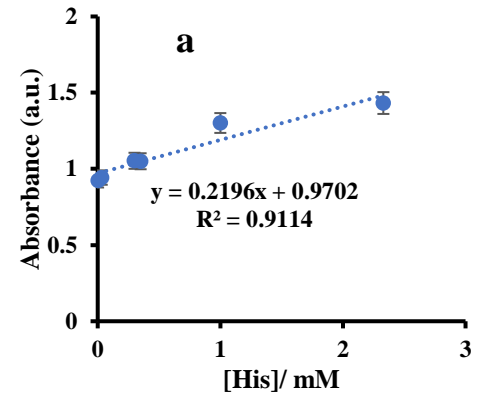
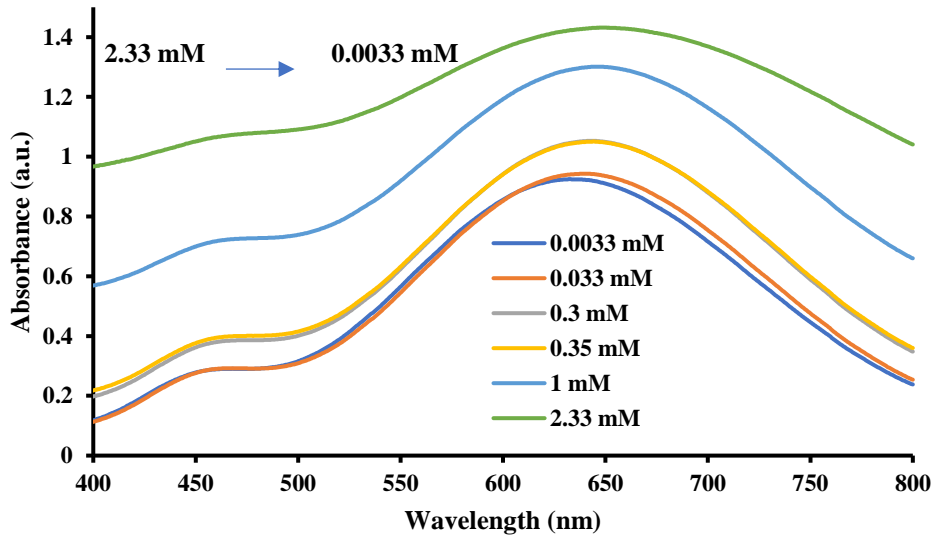


Figure S5. Optimization of additive-probe volume ratio, **A)** control, **B)** control after 1h; **C)** His, **D)** His after 1h; and **E)** EDA, **F)** EDA after 1h. (a-f) Histogram of Abs (a.u.) *versus* additive-probe volume ratio.



A



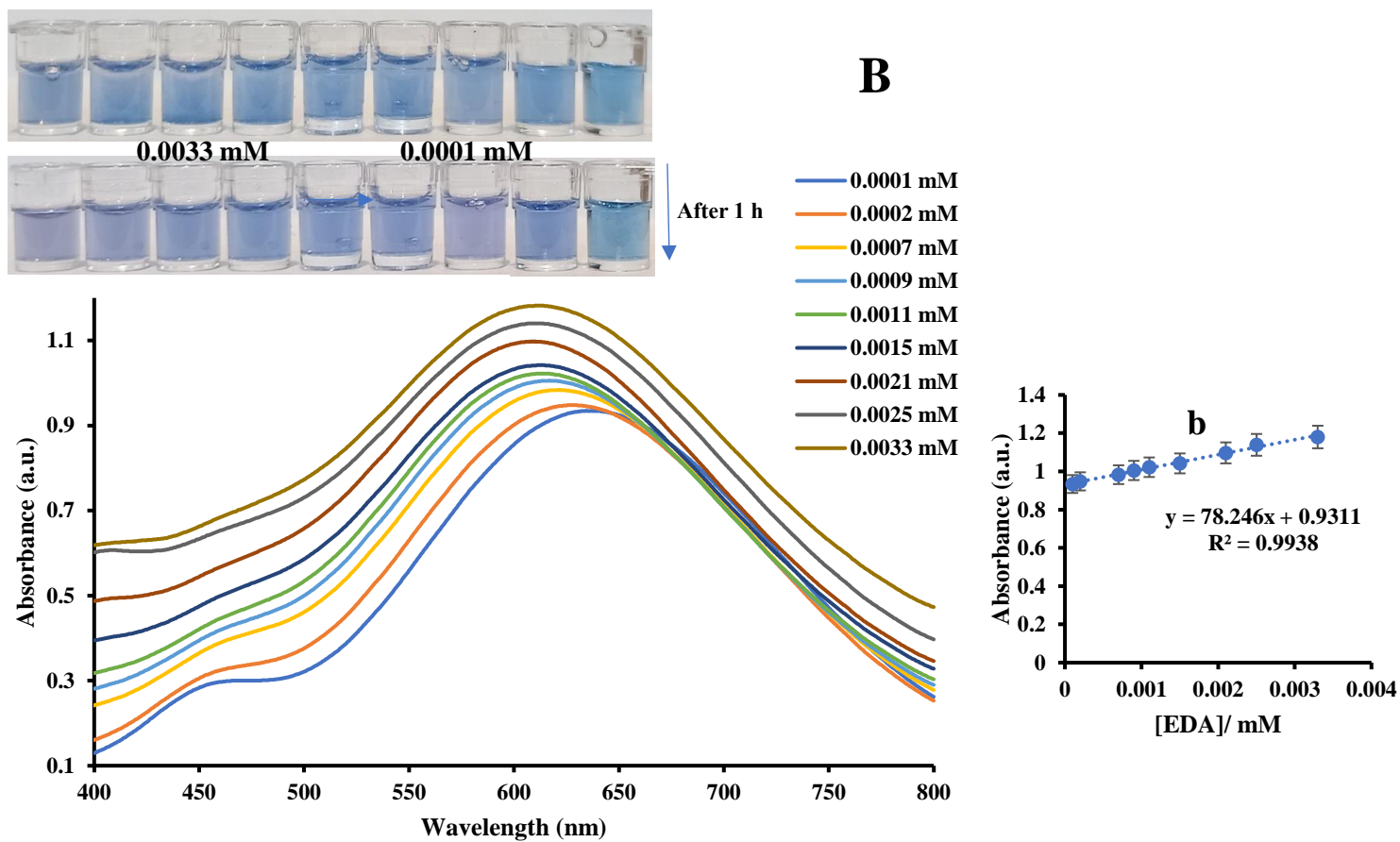
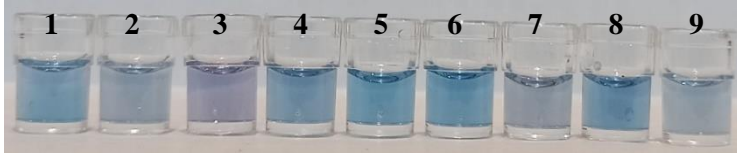
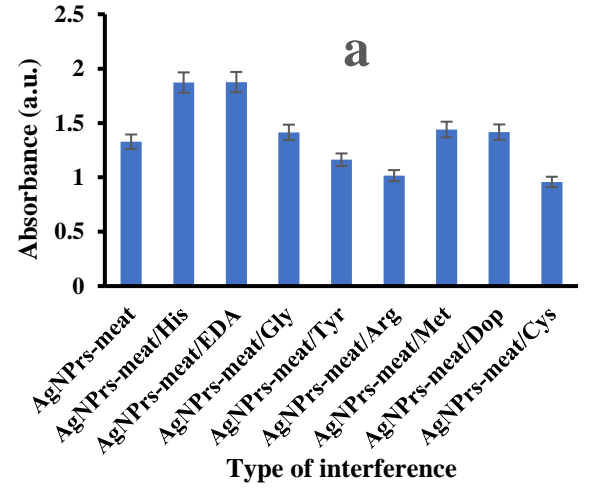
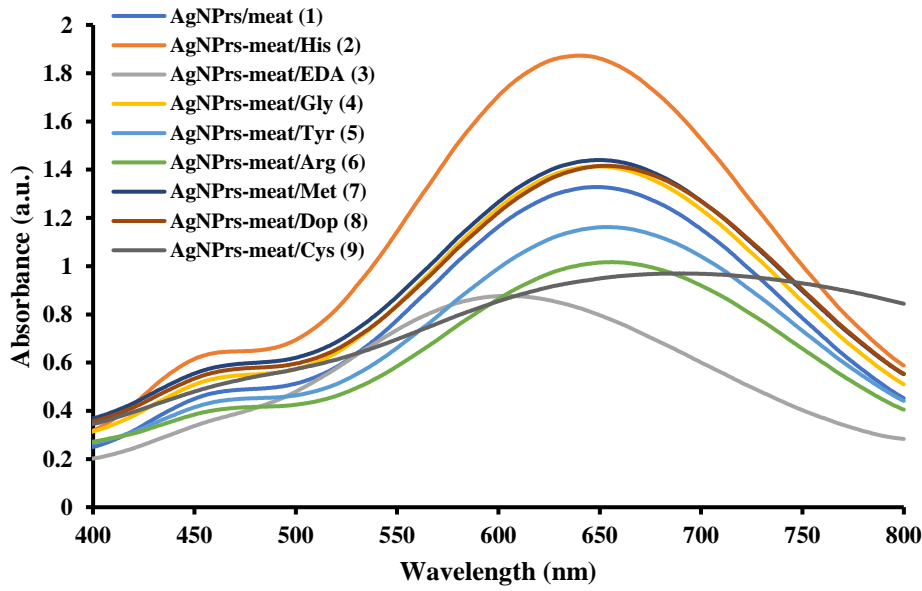


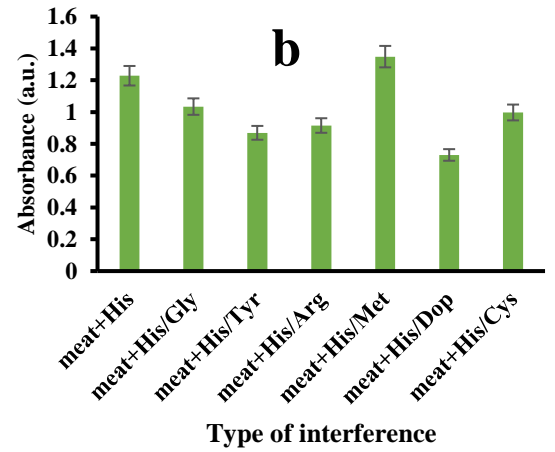
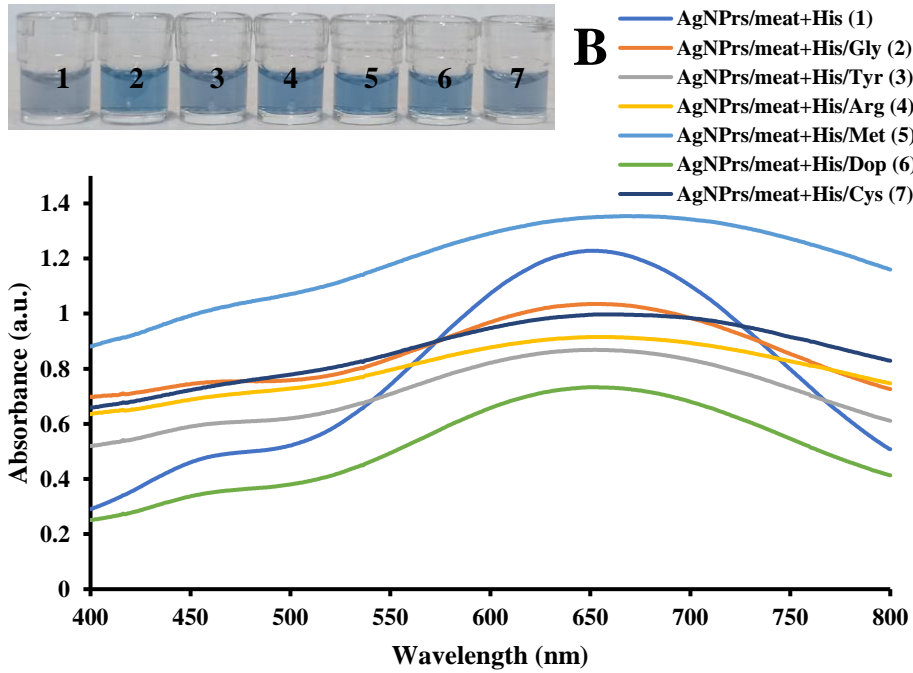
Figure S6. The UV-Vis spectra of AgNPs in the presence of different concentration of (A) HIS (B) EDA at the spoiled meat.



A



B



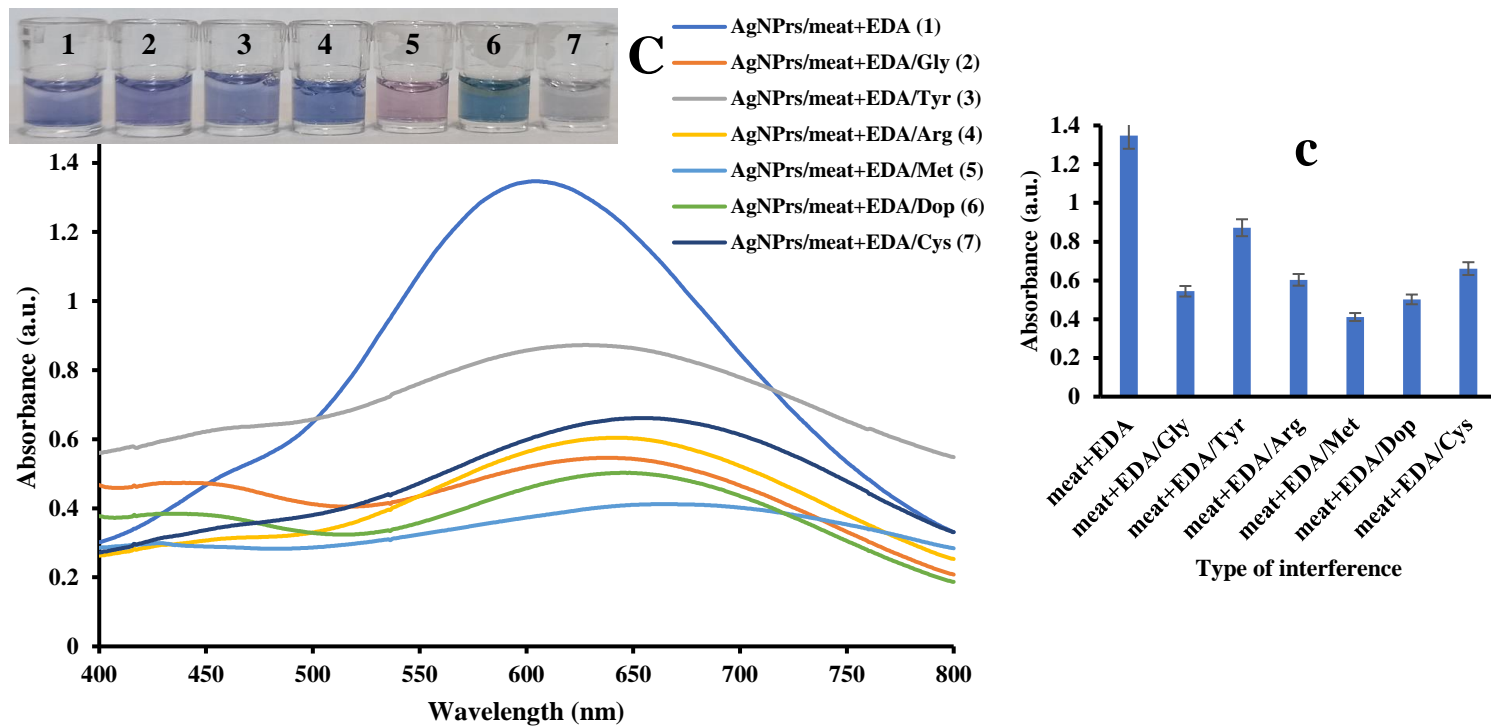
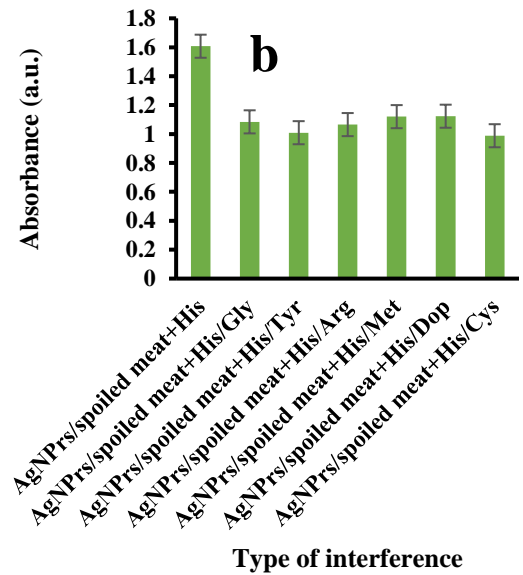
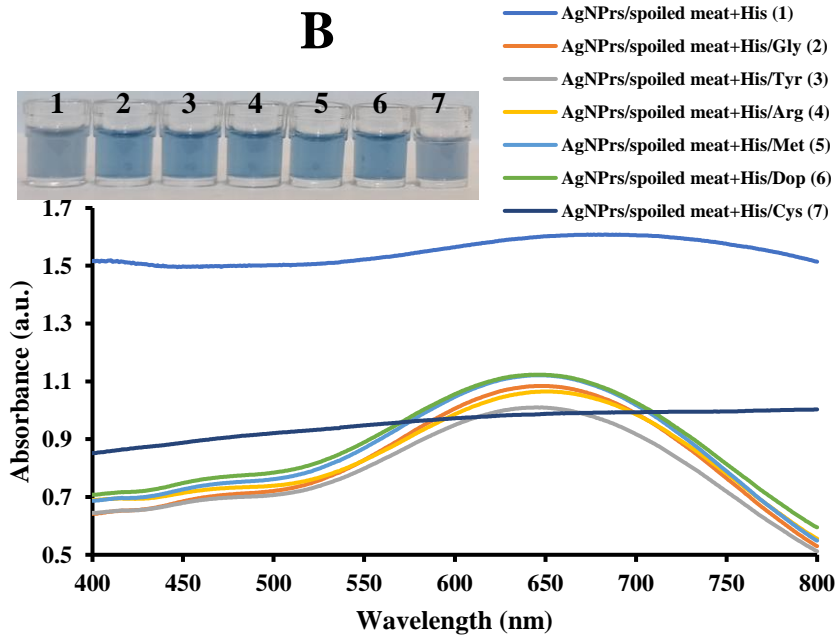
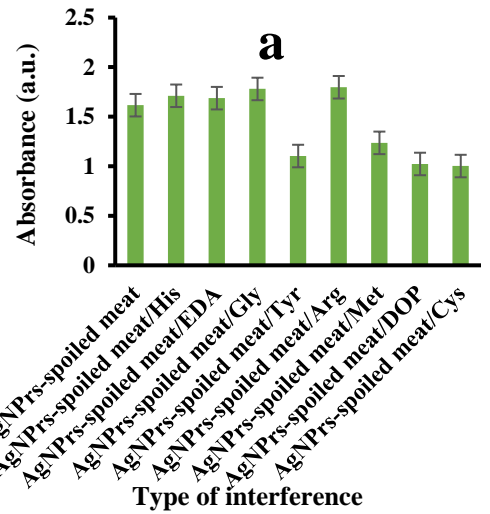
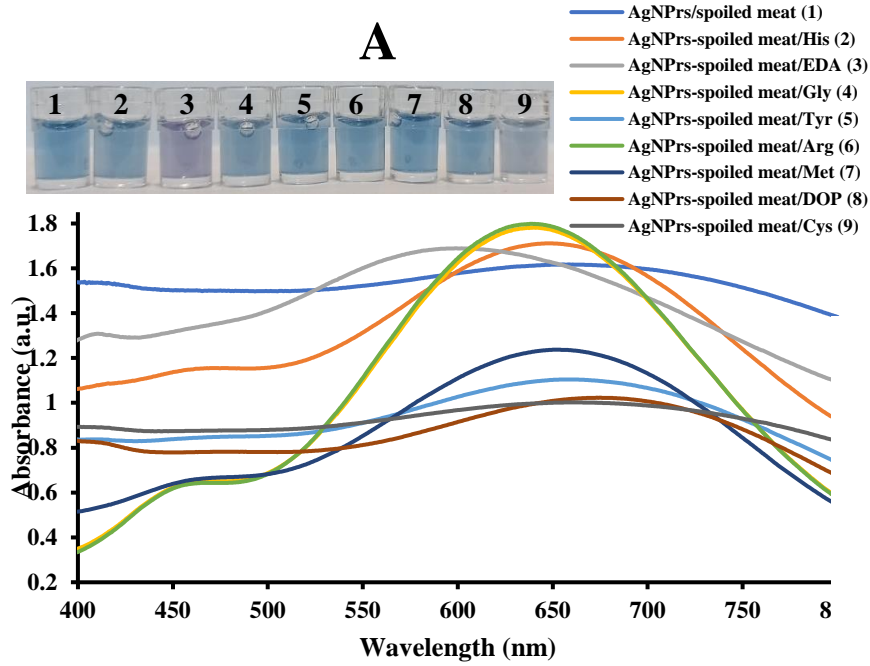


Figure S7. The UV-Vis spectra of AgNPrs in the presence of different interferences (A), different interferences in the presence of HIS (B), and various interferences in the presence of EDA (C) at the fresh meat.



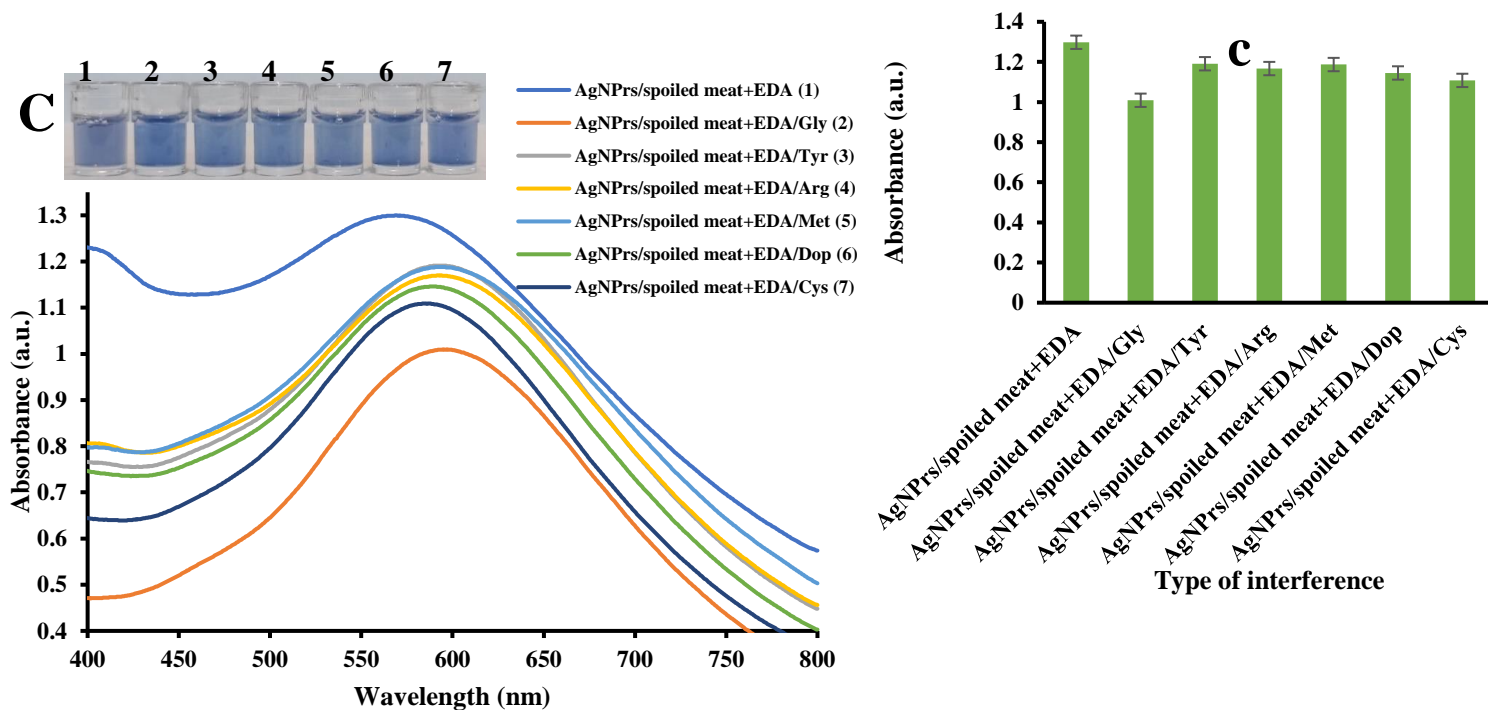


Figure S8. The UV-Vis spectra of AgNPrs in the presence of different interferences (A), various interferences in the presence of HIS (B), and diverse interferences in the presence of EDA (C) at the spoiled meat.

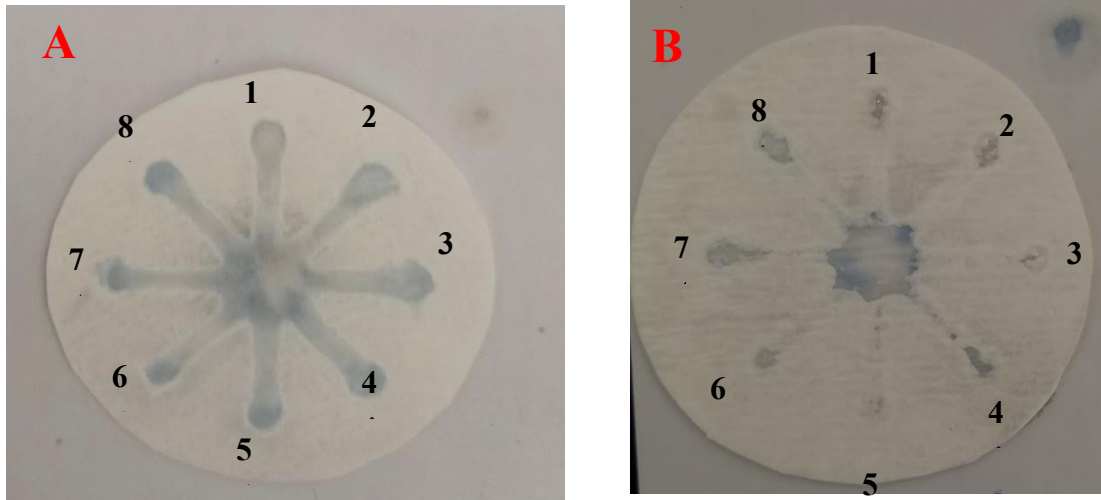


Figure S9. Photographic images of CATS modified by AgNPrs for detection of different concentration of **(A)** His (zones 1 to 8 corresponding to the concentrations of 0.001, 0.0033, 0.01, 0.033, 0.35, 1.35, 2.33, and 3.33 mM, respectively) and **(B)** EDA (zones 1 to 8 corresponding to the concentrations of 0.0001, 0.0002, 0.0004, 0.0009, 0.0015, 0.0021, 0.0025, and 0.0033 mM, respectively) in meat.